J. Am. Chem. Soc. 1994, 116, 7123–7128 7123

Vibrational Spectra and Mutual Ligand Interactions in the Hydrogen-Substituted Main Group Hexafluorides HPF_5^- and HSF_5[†]

Karl O. Christe,[*,1] David A. Dixon,[2] and William W. Wilson[1]

Contribution from Rocketdyne, A Division of Rockwell International Corporation, Canoga Park, California 91309, and the DuPont Corporation, Central Research and Development, Experimental Station, Wilmington, Delaware 19880-0328

Received February 2, 1994[⊗]

Abstract: The new HPF_5^- salt, $N(CH_3)_4HPF_5$, was prepared and the infrared and Raman spectra of $N(CH_3)_4HPF_5$ and $CsHPF_5$ were recorded. The spectra were assigned with the help of ab initio molecular orbital and local density functional calculations, and a normal coordinate analysis was carried out. For comparison, the unknown isoelectronic molecule HSF_5 was also calculated by the same methods. The internal stretching force constants of HPF_5^- are compared to those of closely related phosphorus and sulfur fluorides and hydrides and confirm the existence of a *cis*-effect in these hydrogen-substituted main group hexafluorides. The observed substitution effects are explained in terms of a hypervalent bonding scheme and result in a preferential weakening of the four equatorial *cis*-bonds.

Introduction

During recent studies of the novel PF_4^- anion[3] and its reaction chemistry,[4] the HPF_5^- anion was observed as one of the reaction products. Although this anion is known and has been characterized by ^1H, ^{19}F, and ^{31}P NMR spectroscopy,[5–10] the reports on its vibrational spectra were limited to an incomplete listing of some of the infrared bands without assignments.[8] Since the HPF_5^- anion is the only known main group element species containing five fluorine ligands and one hydrogen ligand, it offered a unique opportunity to examine experimentally the mutual ligand interaction effects exercised by the hydrogen ligand on fluorines in *cis*- and *trans*-positions.

Mutual ligand interaction effects in monosubstituted main group element hexafluorides have been the subject of several previous studies.[11–13] For example, Armstrong and co-workers published in 1975 the results from CNDO/MO calculations on monosubstituted tellurium hexafluorides, TeF_5X. They concluded that generally the four fluorine ligands in *cis*-positions to X become more labile than the one in the *trans*-position, except for $HTeF_5$ where the hydrogen substitution produced a weaker *trans* Te–F bond and, surprisingly, exhibited the weakest ligand interaction within the H, OH, NH_2, Cl, CH_3, Br, SH, PH_2, and SiH_3 series of ligands.[11] In 1976, Shustorovich and Buslaev proposed the terms *trans*- or *cis*-effect, depending on which bond is more strongly affected by the substitution.[12] On the basis of qualitative MO arguments, they predicted for MF_5X compounds, where the main group central atom M is in its highest oxidation state and X is a strong σ donor such as H or CH_3, a *cis*-effect consisting of a weakening of the *cis* M–F bonds and a strengthening of the *trans* M–F bond. They also used the difference Δ between equatorial and axial M–F bond lengths for distinguishing a *cis*-effect from a *trans*-effect. If Δ is positive, the *cis*-effect dominates, while for a negative Δ the *trans*-effect prevails. In 1987, Oberhammer and co-workers determined the structure of SF_5Br by a combined electron diffraction–microwave study and established the presence of a small *cis*-effect. They also carried out ab initio calculations with various basis sets (3-21G, 3-21G*, and 6-31G*) for SF_6 and HSF_5 to confirm the *cis*-effect of a donating substituent in these monosubstituted sulfur hexafluorides but for HSF_5 reported only the calculated bond lengths and angles.[13]

Experimental Section

Apparatus and Materials. Volatile materials were handled in a passivated (with ClF_3) stainless steel–Teflon FEP vacuum line.[14] Nonvolatile materials were handled in the dry nitrogen atmosphere of a glovebox. The infrared, Raman, and NMR spectrometers have previously been described.[3] Literature methods were used for the synthesis of $N(CH_3)_4F$[15] and the drying of HF,[16] CH_3CN,[17] and CsF.[18] The PF_3 (Ozark Mahoning) was purified by fractional condensation prior to its use.

Syntheses of $N(CH_3)_4HPF_5$ and $CsHPF_5$. Typically, 2 mmol of MF ($M = N(CH_3)_4$ or Cs) was loaded in the drybox into a prepassivated 0.75 in. o.d. Teflon FEP ampule that was closed by a stainless steel valve. On the vacuum line, about 4 mL of liquid HF was added and the mixture was agitated at room temperature for 1 h. The excess of unreacted HF was pumped off at room temperature leaving behind $MHF_2{\cdot}nHF$ ($n = 1$–2). Dry CH_3CN (about 3 mL of liquid) and PF_3 (about 6 mmol) were added to the ampule at -196 °C, and the mixture was agitated at room temperature for 1 h which resulted in the precipitation of a white solid. All volatile material was pumped off at room temperature leaving behind $MHPF_5$ in quantitative yield (found weights were within 1 mg of those

---

[†] Dedicated to Prof. Wolfgang Sawodny on the occasion of his 60th birthday.

[⊗] Abstract published in *Advance ACS Abstracts*, June 15, 1994.

(1) Rocketdyne.

(2) DuPont, Contribution No. 6825.

(3) Christe, K. O.; Dixon, D. A.; Mercier, H. P. A.; Sanders, J. C. P.; Schrobilgen, G. J.; Wilson, W. W. *J. Am. Chem. Soc.*, in press.

(4) Christe, K. O.; Dixon, D. A.; Sanders, J. C. P.; Schrobilgen, G. J.; Wilson, W. W., to be submitted for publication.

(5) Nixon, J. F.; Swain, J. R. *Inorg. Nucl. Chem. Lett.* **1969**, *5*, 295.

(6) Nixon, J. F.; Swain, J. R. *J. Chem. Soc. A* **1970**, 2075.

(7) McFarlane, W.; Nixon, J. F.; Swain, J. R. *Mol. Phys.* **1970**, *19*, 141.

(8) Cowley, A. H.; Wisian, P. J.; Sanchez, M. *Inorg. Chem.* **1977**, *16*, 1451.

(9) Minkwitz, R.; Liedtke, A. *Z. Naturforsch. B* **1989**, *44B*, 679.

(10) Lindemann, D.; Riesel, L. *Z. Anorg. Allg. Chem.* **1992**, *615*, 66. Riesel, L.; Kant, M. *Z. Chem.* **1984**, *24*, 382.

(11) Armstrong, D. R.; Fraser, G. W.; Meikle, G. D. *Inorg. Chem. Acta* **1975**, *15*, 39.

(12) Shustorovich, E. M.; Buslaev, Yu. A. *Inorg. Chem.* **1976**, *15*, 1142.

(13) Christen, D.; Mack, H. G.; Oberhammer, H. *J. Chem. Phys.* **1987**, *87*, 2001.

(14) Christe, K. O.; Wilson, R. D.; Schack, C. J. *Inorg. Synth.* **1986**, *24*, 3.

(15) Christe, K. O.; Wilson, W. W.; Wilson, R. D.; Bau, R.; Feng, J. *J. Am. Chem. Soc.* **1990**, *112*, 7619.

(16) Christe, K. O.; Wilson, R. D.; Schack, C. J. *J. Fluorine Chem.* **1978**, *11*, 71.

(17) Christe, K. O.; Dixon, D. A.; Mahjoub, A. R.; Mercier, H. P. A.; Sanders, J. C. P.; Seppelt, K.; Schrobilgen, G. J.; Wilson, W. W. *J. Am. Chem. Soc.* **1993**, *115*, 2696.

(18) Christe, K. O.; Wilson, W. W.; Bau, R.; Bunte, S. W. *J. Am. Chem. Soc.* **1992**, *114*, 3411.

0002-7863/94/1516-7123$04.50/0

Table 1. Vibrational Spectra of $CsHPF_5$ and $N(CH_3)_4HPF_5$ and Their Assignments

obsd freq, cm^{-1} (rel intens)				assignment (point group)	
$CsHPF_5$		$N(CH_3)_4HPF_5$			
IR	Raman	IR	Raman	HPF_5^- (C_{4v})	$N(CH_3)_4^+$ (T_d)
		3130 w			
		3047 m	3046 (25)		
			3004 (9)		$\nu_5(E)$
			2988 sh		
		2975 w	2968 (15)		$\nu_{14}(F_2)$
			2927 (6)		$\nu_1(A_1)$
			2888 (2)		+combination
			2821 (5)		bands
2508 sh					
2478 m		2487 ms	2486 (4)	$2\nu_8(A_1)$	
2378 s		2375 s	2373 (8)		
2360 sh		2355 m	2355 (4)	$\nu_1(A_1)$	
			1530 (1)		
		1494 vs			$\nu_{15}(F_2)$
			1470 (85)		$\nu_2(A_1)$, $\nu_6(E)$
		1442 w			
		1419 ms	1418 (7)		$\nu_{16}(F_2)$
		1303 w			
		1287 w	1287 (3)		$\nu_{17}(F_2)$
1235 vs		1238 vs	1238 (11)	$\nu_8(E)$	
			1175 (8)		$\nu_7(E)$
		949 vs	948 (100)		$\nu_{18}(F_2)$
945 vw				$(\nu_3 + \nu_{11})(E)$	
		918 vw	918 (2)		$2\nu_{19}(F_2)$
740–840 vs, br		750–820 vs, br	800 (3)	$\nu_9(E)$	
762 vs	769 (65)		768 (15)	$\nu_2(A_1)$	
			754 (47)		
			740 sh		$\nu_3(A_1)$
672 vw		672 vw		$2\nu_{11}(A_1)$	
602 s	607 (100)	602 s	608 (20)	$\nu_3(A_1)$	
		579 vw			
558 ms		558 ms	558 (3)	$\nu_4(A_1)$	
	542 (30)	537 vw	542 (6)	$\nu_5(B_1)$	
512 s	514 (25)	512 s	514 (7)	$\nu_{10}(E)$	
		458 mw	458 (15)		$\nu_{19}(F_2)$
	440 (25)		440 (7)	$\nu_7(B_2)$	
			373 (18)		$\nu_8(E)$
333 mw		333 mw	337 (1)	$\nu_{11}(E)$	

calculated for $MHPF_5$). The products were identified by vibrational and NMR spectroscopy as $MHPF_5$ salts.[4–10]

Computational Methods. The geometries, vibrational frequencies, and force fields of HPF_5^- and HSF_5 were calculated, as previously described,[19] in the local density functional (LDF) approximation by using the program system DMol with a polarized double numerical basis set. Ab initio molecular orbital calculations were also performed with the program GRADSCF[20] with a polarized double-ζ basis set and with a polarized double-ζ basis set augmented with a set of diffuse p functions on the heavy atoms and a diffuse s function on hydrogen with $\zeta(s) = 0.041$.[21]

Results and Discussion

Syntheses of the HPF_5^- Salts. Attempts to prepare the HPF_5^- salts from the corresponding fluorides and excess PF_3 in anhydrous HF solution were unsuccessful and resulted in the exclusive formation of the corresponding bifluorides. This is attributed to HF being a stronger Lewis acid than HPF_4 and, therefore, displacing HPF_4 from its HPF_5^- salts. Consequently, the syntheses of the HPF_5^- salts were advantageously carried out in two separate steps. The first one involved the conversion of the fluorides to the bifluorides in anhydrous HF solution,

$$MF + HF \xrightarrow{HF} MHF_2$$

followed by removal of the unreacted HF and the reaction of the resulting bifluoride with PF_3 in CH_3CN solution.

$$MHF_2 + PF_3 \xrightarrow{CH_3CN} MHPF_5$$

This approach offers the additional advantage that for M being cesium, the $CsHF_2$ is quite soluble in CH_3CN while CsF is not. The purity of the $MHPF_5$ salts prepared in this manner is excellent and the yields are quantitative. The use of an excess of PF_3 in this reaction is important to ensure that all MHF_2 is converted to $MHPF_5$ and any excess HF is converted to HPF_4.

Vibrational Spectra of $N(CH_3)_4HPF_5$ and $CsHPF_5$. The infrared and Raman spectra of these two HPF_5^- salts were recorded. The observed frequencies and their assignments are

---

(19) (a) Christe, K. O.; Wilson, R. D.; Wilson, W. W.; Bau, R.; Sukumar, S.; Dixon, D. A. *J. Am. Chem. Soc.* **1991**, *113*, 3795. (b) Dixon, D. A.; Andzelm, J.; Fitzgerald, G.; Wimmer, E.; Jasien, P. In *Density Functional Methods in Chemistry*; Labanowski, J., Andzelm, J., Eds.; Springer Verlag: New York, 1991; p 33. (c) Dixon, D. A.; Christe, K. O. *J. Phys. Chem.* **1992**, *96*, 1018. (d) Delley, B. *J. Chem. Phys.* **1990**, *92*, 508. Dmol is available commercially from BIOSYM Technologies, San Diego, CA. A FINE grid was used.

(20) (a) GRADSCF is an ab initio program system designed and written by A. Komornicki at Polyatomics Research. (b) Komornicki, A.; Ishida, K.; Morokuma, K.; Ditchfield, R.; Conrad, M. *Chem. Phys. Lett.* **1977**, *45*, 595. (c) McIver, J. W., Jr.; Komornicki, A. *Chem. Phys. Lett.* **1971**, *10*, 202. (d) Pulay, P. In *Applications of Electronic Structure Theory*; Schaefer, H. F., III, Ed.; Plenum Press: New York, 1977; p 153. (e) King, H. F.; Komornicki, A. *J. Chem. Phys.* **1986**, *84*, 5465. (f) King, H. F.; Komornicki, A. In *Geometrical Derivatives of Energy Surfaces and Molecular Properties*; Jorgenson, P., Simons, J., Eds.; D. Reidel: Dordrecht, 1986; NATO ASI Series C, Vol. 166, p 207.

(21) (a) For F, H, and O basis sets and for diffuse functions see: Dunning, T. H., Jr.; Hay, P. J. In *Methods of Electronic Structure Theory*; Schaefer, H. F., III, Ed.; Plenum Press: New York, 1977; Chapter 1. (b) For P and S basis sets see: (b) McLean, A. D.; Chandler, G. S. *J. Chem. Phys.* **1980**, *72*, 5639.

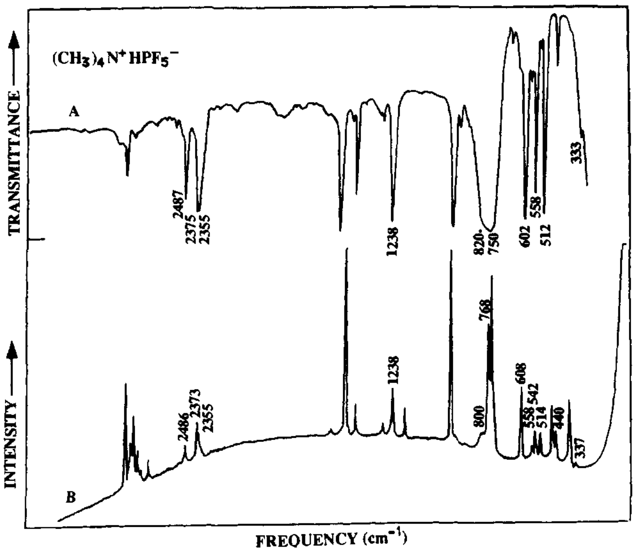

Figure 1. Infrared (A) and Raman (B) spectra of solid $N(CH_3)_4HPF_5$ recorded at room temperature. The bands due to the anion are marked by their frequency values.

summarized in Table 1. The spectra of $N(CH_3)_4HPF_5$ were of better quality than those of $CsHPF_5$ and are shown in Figure 1. The bands due to HPF_5^- are marked by their frequency values; the remaining bands belong to the $N(CH_3)_4^+$ cation.

The assignments for the $N(CH_3)_4^+$ cation are well understood[3,15,17] and were made accordingly. The assignments for HPF_5^- were made in point group C_{4v}, based on frequency and intensity arguments, and above all a comparison with the results from the local density functional and ab initio calculations (see below). The agreement between the observed and calculated frequencies is very good and firmly establishes the assignments given in Tables 1 and 2.

Ab Initio Electronic Structure Theory Calculations. Ab initio molecular orbital (MO) theory and LDF theory were used to calculate the vibrational frequencies (Table 2), geometries (Table 3), force fields (Table 4), and potential energy distributions (Table 5) for the HPF_5^- anion and the isoelectronic HSF_5 molecule. The LDFT vibrational frequencies calculated for HPF_5^- are in excellent agreement with the experimentally observed ones after scaling of the deformation modes by an empirical factor of 1.1012 to maximize the fit. The scaling of the deformation frequencies is necessary because the bond lengths, calculated at the LDFT level, tend to be long by about 0.02–0.05 Å for these types of compounds[3] and the deformation frequencies are more strongly influenced by the bond length changes than the stretching modes. The MO results also show very good agreement with the experimental frequencies if empirical scaling factors are used. In general, the MO methods tend to underestimate bond lengths so that the frequencies are overestimated. It is also worth noting that the calculated values are harmonic and anharmonicity lowers the observed frequencies. The MO bond lengths are about 0.04 Å shorter than the corresponding LDFT values for HPF_5^-, whereas for HSF_5, the differences increase to about 0.05 Å. The calculated angles agree with each other. There is only a small effect of adding diffuse functions to the basis set at the MO level on the frequencies and there is no effect within 0.001 Å on the geometries. Furthermore, the S–F bond lengths calculated by us for HSF_5 at the HF/DZP+ level of theory are in good agreement with those previously obtained[13] at the 3-21G* and 6-31G* levels. The quality of our LDFT and HF/DZP+ methods was also examined by calculating the geometries of the closely related PF_6^- and SF_6 species for which experimental values are known.[22,23] The results from the calculations are given in Table 3 and the following predictions can be made for the actual geometries of HPF_5^- and HSF_5: HPF_5^-, $r(P–F_{ax}) = 1.628$ Å, $r(P–F_{eq}) = 1.649$ Å, $r(P–H) = 1.404$ Å, $\angle(F_{ax}–P–F_{eq}) = 89.3°$; HSF_5, $r(S–F_{ax}) = 1.574$ Å, $r(S–F_{eq}) = 1.586$ Å, $r(S–H) = 1.324$ Å, $\angle(F_{ax}–S–F_{eq}) = 89.5°$.

Structure and Bonding in HPF_5^- and HSF_5. The species HPF_5^- and HSF_5 can be derived from octahedral PF_6^- and SF_6, respectively, by substitution of one fluorine ligand by one hydrogen ligand. Since no experimental data were available on how hydrogen substitution in a perfluorinated XF_6 species influences the rest of the molecule,[12,24] it was interesting to analyze this situation more closely.

First, consider the repulsion effects of the hydrogen ligand. According to the second basic tenet of the valence shell electron pair domain (VSEPD) model,[25] the size of a single bond domain in the valence shell of a central atom decreases with increasing electronegativity of the ligand. Since hydrogen has a much lower electronegativity than fluorine, the electron pair domain of a P–H bond should be larger than that of a P–F bond and, therefore, a P–H bond domain should be more repulsive than that of a P–F bond. As has already previously been pointed out, this tenet is not generally valid, as was shown by the bond angles of PH_3 and PF_3 and 30 additional examples.[26] Contrary to the VSEPD expectations, the bond angle in PF_3 (97.8°) is significantly larger than that in PH_3 (93.8°), suggesting that the size of the ligands is also important.[26] On the basis of general considerations, one

Table 2. Comparison of Observed and Calculated Frequencies of HPF_5^- and Calculated Frequencies of HSF_5 and Their Approximate Mode Descriptions

IR and Raman activity	assignmt in Pt group C_{4v}		approx mode description	HPF_5^-					HSF_5[d]		
				obsd freq, cm^{-1} (int)		calcd freq, cm^{-1} (IR int)			calcd freq, cm^{-1} (IR int)[e]		
				IR	Raman	LDFT/DNP[a]	HF/DZP[b]	HF/DZP+[c]	LDFT/DNP	HF/DZP	HF/DZP+
IR, RA	A_1	ν_1	ν XH	2375 s	2373 (8)	2368	2367 (244)	2394 (246)	2661	2756 (17)	2727 (14)
		ν_2	ν XF_{ax}	762 vs	768 (15)	773	793 (268)	794 (277)	821	875 (261)(	867 (263)
		ν_3	ν sym XF_4 in phase	602 s	608 (20)	591	599 (45)	598 (52)	652	688 (32)	681 (34)
		ν_4	δ umbrella XF_4	558 ms	558 (3)	571	556 (25)	556 (22)	619	619 (42)	618 (41)
–, RA	B_1	ν_5	ν sym XF_4 out of phase		542 (6)	538	528 (0)	526 (0)	603	629 (0)	622 (0)
		ν_6	δ pucker, XF_4		not obsd	281	287 (0)	288 (0)	314	328 (0)	327 (0)
–, RA	B_2	ν_7	δ sciss XF_4		440 (7)	436	432 (0)	432 (0)	487	492 (0)	489 (0)
IR, RA	E	ν_8	δ wag XH	1238 vs	1238 (11)	1236	1293 (144)	1288 (128)	1328	1420 (25)	1411 (27)
		ν_9	ν asym XF_4	750–820 vs	800 (3)	801	803 (1070)	798 (1158)	890	923 (1080)	912 (1124)
		ν_{10}	δ wag XF_{ax}	512 s	514 (7)	510	505 (27)	505 (28)	556	565 (40)	562 (39)
		ν_{11}	δ asym XF_4 in plane	333 mw	337 (1)	331	333 (1.7)	334 (1.5)	371	385 (4.8)	383 (4.6)

[a] The deformation frequencies were multiplied by a factor of 1.1012 to maximize their fit with their observed frequencies. [b] The stretching and deformation frequencies were multiplied by factors of 0.90624 and 0.92748, respectively. [c] The stretching and deformation frequencies were multiplied by factors of 0.89874 and 0.92345, respectively. [d] In the absence of experimental data, the same scaling factors as for HPF_5^- were used. [e] In km mol^{-1}.

Table 3. Calculated Geometries of HPF_5^- and HSF_5 Compared to Those Calculated and Observed for PF_6^- and SF_6

	HPF_5^-		HSF_5				
	LDFT/DNP	HF/DZP+	LDFT/DNP	HF/DZP+	3-21G*[a]	6-31G*[a]	MP2/6-31G*[a]
$r(X-F_{ax})$	1.642	1.607	1.602	1.553	1.556	1.560	1.602
$r(X-F_{eq})$	1.662	1.628	1.613	1.567	1.565	1.573	1.611
$r(X-H)$	1.418	1.382	1.351	1.305			
$\angle(F_{ax}-X-F_{eq})$	89.3	89.3	89.6	89.5	89.3	89.4	89.4

	PF_6^-			SF_6				
	obsd[b]	LDFT/DNP	HF/DZP+	obsd[c]	LDFT/DNP	HF/DZP+	3-21G*[a]	6-31G*[a]
$r(X-F)$	1.625	1.639	1.603	1.563	1.593	1.548	1.550	1.554

[a] Values from ref 13. [b] Values from ref 23. [c] Values from ref 22.

Table 4. Scaled[a] LDFT/DNP and HF/DZP+ Force Fields[b] of HPF_5^- and HSF_5

HPF_5^-

	A$_1$					B$_1$			E			
	F_{11}	F_{22}	F_{33}	F_{44}		F_{55}	F_{66}		F_{88}	F_{99}	$F_{10,10}$	$F_{11,11}$
F_{11}	3.228 (3.247)				F_{55}	3.234 (3.034)		F_{88}	0.873 (0.892)			
F_{22}	−0.003 (−0.001)	4.018 (4.109)			F_{66}	−0.131 (−0.096)	1.116 (1.228)	F_{99}	0.444 (0.469)	3.597 (3.605)		
						B$_2$						
F_{33}	0.184 (0.330)	0.580 (0.803)	4.218 (4.341)		F_{77}	1.467 (1.373)		$F_{10,10}$	0.050 (0.060)	0.515 (0.554)	1.724 (1.627)	
F_{44}	−0.119 (−0.137)	0.744 (0.778)	−0.095 (−0.029)	2.154 (1.988)				$F_{11,11}$	0.108 (0.113)	0.393 (0.431)	0.217 (0.192)	1.649 (1.577)

HSF_5

	A$_1$					B$_1$			E			
	F_{11}	F_{22}	F_{33}	F_{44}		F_{55}	F_{66}		F_{88}	F_{99}	$F_{10,10}$	$F_{11,11}$
F_{11}	4.062 (4.267)				F_{55}	4.062 (4.316)		F_{88}	0.917 (0.968)			
F_{22}	−0.103 (−0.043)	4.626 (5.188)			F_{66}	−0.183 (−0.151)	1.450 (1.480)	F_{99}	0.488 (0.537)	4.467 (4.800)		
						B$_2$						
F_{33}	0.002 (0.017)	0.408 (0.687)	4.952 (5.520)		F_{77}	1.728 (1.650)		$F_{10,10}$	0.042 (0.066)	0.537 (0.624)	1.952 (1.918)	
F_{44}	0.039 (0)	0.810 (0.890)	−0.195 (−0.095)	2.431 (2.270)				$F_{11,11}$	0.090 (0.097)	0.448 (0.505)	0.223 (0.194)	1.928 (1.887)

[a] For the LDFT/DNP force fields, the deformation constants were scaled by a factor of $(1.1012)^2$ and the stretch–bend interaction constants by 1.1012. For the HF/DZP+ force fields, the following scaling factors were used: stretching constants, $(0.89874)^2$; deformation constants, $(0.92345)^2$; and stretch–bend interaction constants (0.89874×0.92345). [b] The HF/DZP+ force fields are listed in parentheses.

Table 5. Potential Energy Distributions for HPF_5^- and HSF_5 for the LDFT/DNP Force Field

		HPF_5^-		HSF_5	
		freq, cm^{-1}	PED, %	freq, cm^{-1}	PED, %
A$_1$	ν_1	2368	$99.6S_1$	2661	$99.5S_1 + 0.3S_4 + 0.1S_2$
	ν_2	773	$53.3S_2 + 42.0S_4 + 4.7S_3$	821	$51.7S_2 + 45.2S_4 + 2.9S_3 + 0.2S_1$
	ν_3	591	$73.0S_3 + 14.1S_4 + 12.6S_2 + 0.35S_1$	652	$84.1S_3 + 11.2S_2 + 4.7S_4$
	ν_4	571	$92.3S_4 + 7.4S_2 + 0.2S_3$	619	$92.9S_4 + 6.7S_2 + 0.3S_3 + 0.1S_1$
B$_1$	ν_5	538	$99.9S_5 + 0.1S_6$	603	$99.8S_5 + 0.2S_6$
	ν_6	281	$99.8S_6 + 0.2S_5$	315	$99.7S_6 + 0.3S_5$
B$_2$	ν_7	436	$100S_7$	487	$100S_7$
E	ν_8	1236	$99.9S_8$	1328	$99.9S_8$
	ν_9	801	$59.6S_9 + 17.4S_{11} + 13.9S_8 + 9.1S_{10}$	890	$55.5S_9 + 18.7S_8 + 16.9S_{11} + 8.9S_{10}$
	ν_{10}	510	$61.5S_{10} + 29.8S_{11} + 6.9S_8 + 1.8S_9$	556	$60.8S_{10} + 31.7S_{11} + 5.8S_8 + 1.7S_9$
	ν_{11}	331	$59.0S_{11} + 38.0S_{10} + 2.7S_8 + 0.3S_9$	372	$57.7S_{11} + 40.2S_{10} + 1.9S_8 + 0.2S_9$

should expect at least three factors to influence the bond angles in HPF_5^-. These are the sizes of the ligands, the phosphorus–ligand bond distances, and the electronegativities of the ligands which influence the size of the electron pair domains. Since these factors can partially compensate each other,[27] it is difficult to predict the net effect. The slight compression of the F_{ax}–P–F_{eq} bond angle in HPF_5^- (see Table 3) indicates that the effective repulsions from the hydrogen ligand or its bonding electron pair domain are somewhat larger than those from the fluorine ligands but the overall effect is quite small.

Table 6. Internal Stretching Force Constants of HPF_5^- and HSF_5 Compared to Those of Closely Related Pseudooctahedral Species and Some Hydrides

	stretching force constant, mdyn/Å		
compd	M–F_{eq}	M–F_{ax}	M–H
PF_6^- [a]	4.39	4.39	
HPF_5^- [b]	3.66	4.02	3.23
$H_2PF_4^-$ [c]	3.07		3.19
PH_4^+ [d]			3.19
PH_3 [d]			3.10
SF_6 [e]	5.26	5.26	
SF_5Cl [f]	4.51	4.83	
HSF_5 [g]	4.49	4.63	4.06
SF_5Br [h]	4.29	4.50	
SOF_5^- [i]	3.60	3.75	
SF_5^- [k]	2.06	4.12	
H_2S [d]			3.95
H_3S^+ [j]			3.65

[a] Reference 29. [b] This work; frr = 0.246, frr′ = 0.0645. [c] Reference 30. [d] Reference 31. [e] Reference 32. [f] Reference 33. [g] This work; frr = 0.2225, frr′ = 0.020. [h] Reference 34. [i] Reference 35. [k] Reference 36. [j] Reference 37.

The second point of interest concerns the influence of hydrogen substitution on the X–F bond strengths and whether there is a significant *cis*- or *trans*-effect.[12,13] Since hydrogen substitution releases additional electron density into the rest of these molecules, the ($\delta-$)F–X($\delta+$) bond polarities and, hence, the lengths of their X–F bonds should increase. The calculated bond distances clearly show this. In HPF_5^-, the P–F_{ax} distance is essentially the same as that in PF_6^- whereas the P–F_{eq} bond distances are 0.02 Å longer (see Table 3). Another measure of the bond strengths are the internal stretching force constants (see Table 6). The HPF_5^- force constants were derived from the scaled LDFT vibrational frequencies which are almost identical to the experimentally observed ones (see Table 2) and, hence, should be very close to the true force field.[28] As can be seen from Table 6, the averaged P–F stretching force constant decreases, as expected, from PF_6^- (4.39 mdyn/Å)[29] to HPF_5^- (3.73 mdyn/Å). Substitution of a second fluorine ligand by hydrogen, i.e., going from HPF_5^- to *trans*-$H_2PF_4^-$, causes a comparable further weakening of the P–F bonds (*trans*-$H_2PF_4^-$ = 3.07 mdyn/Å).[30] Calculations carried out by us for $H_2PF_4^-$ at the SCF and MP-2 levels of theory with the DZP basis set confirmed this trend and showed that *trans*-$H_2PF_4^-$ is favored over the *cis*-isomer by 5.3 and 6.4 kcal/mol, respectively. This agrees with the previous experimental studies[8,30] on $H_2PF_4^-$ in which only the *trans*-isomer was observed.

Table 6 also shows that in HPF_5^- the *cis*-fluorines are more strongly affected by hydrogen substitution than the *trans*-fluorine. These results confirm the *cis*-effect previously predicted[12] by Shustorovich and Buslaev; however, there is no evidence for a simultaneous shortening of the M–F_{trans} bond. The M–F_{trans} bond is also weakened, although to a lesser extent than the M–F_{cis} bonds. Shustorovich and Buslaev also analyzed correctly[12] that when in MXF_5 the ligand X is multiply bonded such as a terminal oxygen and the *cis*-M–F bonds may be slightly longer than the *trans*-M–F bonds, as shown for SOF_5^- (see Table 6)[35] and recently also for IOF_5.[38]

The following model can account for the main features and ligand interactions in these hypervalent, substituted, pseudooctahedral main group fluorides. Ideally, only s and p orbitals are being used for the central atom requiring the assumption of semi-ionic, 3 center–4 electron (3c–4e) bonds[39] to compensate for the resulting electron deficiency. Since 3c–4e bonds involve one p-orbital of the central atom for binding two fluorine ligands, 3c–4e bonding is possible only for approximately linear FMF groups possessing highly electronegative ligands because each ligand must carry half a negative formal charge. In MXF_5 or *trans*-MX_2F_4 where X is either a sterically active free valence electron pair or a highly electropositive ligand, the ligand X is ill-suited for the formation of a semi-ionic 3c–4e bond and, therefore, seeks high s-character, i.e., increased covalency. As a consequence, the four equatorial M–F_{cis} bonds are favored to form two semi-ionic, 3c–4e bond pairs. Since the axial F ligand which is *trans* to X either cannot, if X is a free valence electron pair, form or is less favored, if X is less electronegative than fluorine, to form a linear semi-ionic, 3c–4e bond pair, it seeks to form a regular covalent M–F bond. This scheme accounts for the very large difference[36] between axial and equatorial bond strengths in SF_5^-, where X is a sterically active free valence electron pair, and the much smaller, but significant, differences in MXF_5 species, where X is either H, Br,[34] or Cl.[33] If X is a doubly bonded ligand, such as a terminal oxygen,[35] the M–O π bond competes with the equatorial semi-ionic bonds for p_x and p_y orbital electron density and, thus, weakens the *cis*-M–F_{eq} bonds. However, this effect appears to be relatively weak.

The M–H stretching force constants are surprisingly insensitive to changes in the ligands, the oxidation state of the central atom, and formal positive or negative charges. Thus, the P–H stretching force constant of PH_4^+ (3.19 mdyn/Å)[31] is almost identical to that found for HPF_5^- (3.23 mdyn/Å), and the same holds for the analogous sulfur compounds (see Table 6).

We would like to briefly comment on HSF_5. Although this molecule is still unknown, the LDF calculations indicate that the molecule is vibrationally stable. We anticipate that the molecule, if prepared, will undergo relatively easy HF elimination to give SF_4 + HF.

Finally, it is interesting to compare the results from this study with the reverse substitution effect, i.e., the influence of one or two fluorine atoms on hydrogen ligands in pseudooctahedral main group compounds. In a previous theoretical study[40] on H_5SbF^-,

---

(22) McDowell, R. S.; Aldridge, J. P.; Holland, R. F. *J. Chem. Phys.* **1976**, *80*, 1203.

(23) Gutsev, G. L. *J. Chem. Phys.* **1993**, *98*, 444.

(24) Gillespie, R. J.; Hargittal, I. *The VSEPR Model of Molecular Geometry*; Allyn and Bacon: Boston, 1991.

(25) Gillespie, R. J. *Can. J. Chem.* **1992**, *70*, 742.

(26) Myers, T. *Monatsh. Chem.* **1992**, *123*, 363.

(27) The partial compensation of the ligand size and bond length effects on the bond angles is demonstrated by the following two examples: (a) NF_3 ∠ 102.2° and r = 1.37 Å, NH_3 ∠ 106.6 and r = 1.01 Å, PF_3 ∠ 97.8° and r = 1.56 Å, PH_3 ∠ 93.8° and r = 1.42 Å; (b) OF_2 ∠ 103.3° and r = 1.41 Å, OH_2 ∠ 104.8° and r = 0.965 Å, SF_2 ∠ 98.3° and r = 1.59 Å, SH_2 ∠ 92.2° and r = 1.34 Å. For the same ligands, but decreasing sizes of the central atoms and hence decreasing bond lengths, the ligand–ligand repulsions and thereby the bond angles increase, i.e., from PF_3 to NF_3, PH_3 to NH_3, SF_2 to OF_2, and SH_2 to OH_2. For the same central atom but different ligands, the size of the ligands and the bond length changes are much smaller than for the second period ones and, therefore, the ligand size effect dominates and the bond angles increase on going from SH_2 to SF_2 and PH_3 to PF_3. For the second period central atoms the relative bond length shortening dominates and, hence, the bond angles increase on going from OF_2 to OH_2 and from NF_3 to NH_3.

(28) The scaled LDF frequencies closely duplicate the experimentally observed ones and LDF force fields generally predict the actual off-diagonal symmetry force constants very well. Therefore, the scaled stretching force constants for HPF_5^- and HSF_5 used for the discussion in this paper should be very good measures for the relative strengths of the axial and equatorial bonds in these species.

(29) Christe, K. O.; Wilson, R. D. *Inorg. Chem.* **1975**, *14*, 694.

(30) Christe, K. O.; Schack, C. J.; Curtis, E. C. *Inorg. Chem.* **1976**, *15*, 843.

(31) Siebert, H. *Anwendungen der Schwingungsspektroskopie in der Anorganischen Chemie*; Springer-Verlag: Berlin, 1966.

(32) Ruoff, A. *J. Mol. Struct.* **1969**, *4*, 332.

(33) Sawodny, W. Habilitation, University of Stuttgart, Germany, 1969.

(34) Christe, K. O.; Curtis, E. C.; Schack, C. J.; Roland, A. *Spectrochim. Acta, Part A* **1977**, *33A*, 69.

(35) Christe, K. O.; Schack, C. J.; Pilipovich, D.; Curtis, E. C.; Sawodny, W. *Inorg. Chem.* **1973**, *12*, 620.

(36) Christe, K. O.; Curtis, E. C.; Schack, C. J.; Pilipovich, D. *Inorg. Chem.* **1972**, *11*, 1679.

(37) Christe, K. O. *Inorg. Chem.* **1975**, *14*, 2230.

(38) Christe, K. O.; Curtis, E. C.; Dixon, D. A. *J. Am. Chem. Soc.* **1993**, *115*, 9655.

(39) (a) Pimentel, G. C. *J. Chem. Phys.* **1951**, *19*, 446. (b) Hach, R. J.; Rundle, R. E. *J. Am. Chem. Soc.* **1951**, *73*, 4321. (c) Rundle, R. E. *J. Am. Chem. Soc.* **1963**, *85*, 112.

(40) Yamamoto, Y.; Fujikawa, H.; Fujishima, H.; Akiba, K. *J. Am. Chem. Soc.* **1989**, *111*, 2276.

H_5SbOH^-, and $H_4SbF_2^-$ it was shown that the electron-withdrawing effect of fluorine dominates and mainly affects the hydrogen in the *trans*-position by increasing the (δ+)H–Sb(δ–) bond polarity and thereby its bond length. Hence, the effect of hydrogen substitution strongly differs from that of fluorine substitution. Whereas fluorine substitution results in a simple, electron-withdrawing and bond-weakening *trans*-effect, hydrogen substitution results in a preferential weakening of the *cis*-ligands due to increased contributions from semi-ionic 3c–4e bonding to the *cis*-bonds.

Acknowledgment. We thank the U.S. Army Research Office and U.S. Air Force Phillips Laboratory for financial support (K.O.C., W.W.W.), Dr. J. Sanders and Prof. G. Schrobilgen for the recording of the HPF_5^- NMR data, and one of the reviewers for bringing the H_5SbF^- work to our attention.